

# Grain Boundary Property Determination through Measurement of Triple Junction Geometry and Crystallography

\*A. D. Rollett<sup>1</sup>, C.-C. Yang<sup>1</sup>, W. W. Mullins<sup>1</sup>, B. L. Adams<sup>5</sup>, C. T. Wu<sup>1</sup>, D. Kinderlehrer<sup>2</sup>, S. Ta'asan<sup>2</sup>, F. Manolache<sup>2</sup>, C. Liu<sup>2</sup>, I. Livshits<sup>2</sup>, D. Mason<sup>4</sup>, A. Talukder<sup>3</sup>, S. Ozdemir<sup>3</sup>, D. Casasent<sup>3</sup>, A. Morawiec<sup>1</sup>, D. Saylor<sup>1</sup>, G. S. Rohrer<sup>1</sup>, M. Demirel<sup>1</sup>, B. El-Dasher<sup>1</sup>, W. Yang<sup>1</sup>

<sup>1</sup>Department of Materials Science and Engineering, Carnegie Mellon University, Pittsburgh, PA 15213-3890.

<sup>2</sup>Department of Mathematical Sciences, Carnegie Mellon University.

<sup>3</sup>Department of Electrical and Computer Engineering, Carnegie Mellon University.

<sup>4</sup>Department of Materials Science and Mechanics, Michigan State University.

<sup>5</sup>Department of Mechanical Engineering, Brigham Young University.

*Keywords:* grain boundary properties, polycrystals, energy, mobility, triple junctions, aluminum.

**Abstract.** Microstructure controls the properties of most useful materials. Thus an ability to control microstructure through the processing of materials is a key to optimization of materials performance. Most materials are polycrystalline and their grain structure is a very important aspect of their microstructure. Thanks to their complexity there is a great variety of grain boundary types even in relatively isotropic materials such as the cubic metals. Simply describing the crystallography requires five (macroscopic) parameters (e.g. disorientation and inclination). Evidently, acquiring a knowledge of the variation of properties such as energy and mobility as a function of grain boundary type would be of great value in predicting properties and optimizing processing. This paper outlines the methods being employed to extract such properties from the geometry and crystallography of triple junctions between grain boundaries.

## 1 Introduction

### 1.a Approach

The aim of this paper is to lay out a procedure, with an example, for measuring the properties of interfaces as a function of their crystallographic character that is capable of characterizing the full range of boundary type. The scope is limited to determination of excess free energy and mobility of homophase interfaces, i.e. grain boundaries in single phase materials. The approach relies on measurement of

the geometry and crystallography of grain boundary junctions i.e. triple points [1], fig. 1.

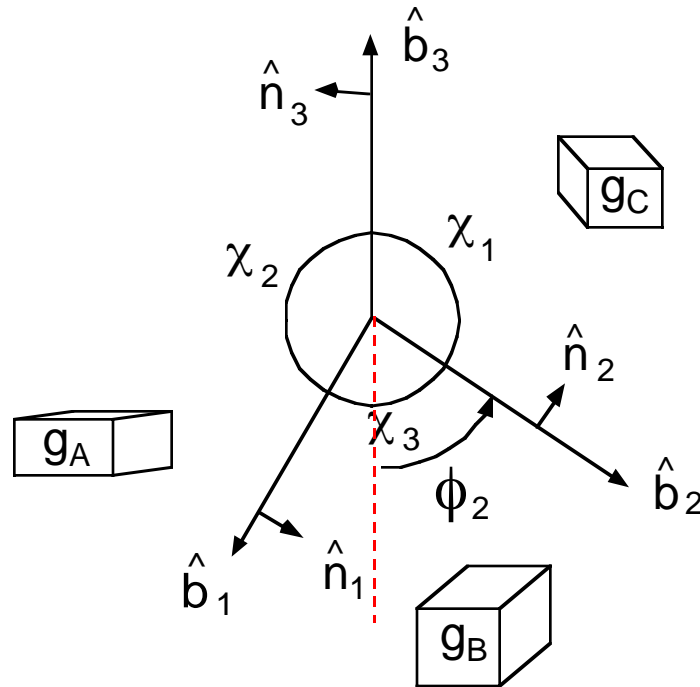


**Fig. 1.** Diagram of a labeling convention for grain boundary character, showing dihedral angles,  $\chi$ , inclination angles,  $\phi$ , boundary tangent vectors,  $\mathbf{b}$ , boundary normals,  $\mathbf{n}$ , and grain orientations,  $g$ . The triple junction line is perpendicular to the plane of the diagram.

In the general case, the crystallographic orientations of each grain, the grain boundary tangents and the triple line tangent are measured with the aid of serial sectioning. For samples in which columnar structures can be generated (typically thin foils or films), the geometry may be measured directly on a single section perpendicular to the column axis. The analytical procedure for extracting properties is statistical and multiscale which means that the number of measurements must be large enough to ensure that each boundary type has been adequately sampled. It is assumed that local equilibrium exists at each triple junction so that the Herring relations (for force balance) may be applied [2]. Each triple junction provides two independent relations between boundary energies. Analysis of the set of relations generates a distribution of boundary energies that (simultaneously) satisfies the Herring relations at each triple junction. The Herring equations [3], describing equilibrium at a triple junction, result from the

requirement that a virtual displacement of the triple junction in any direction causes no first order change in energy. The equations are

$$\sum_{j=1}^3 \left\{ \sigma_j \hat{b}_j + \left( \frac{\partial \sigma_j}{\partial \phi_j} \right) \hat{n}_j \right\} = 0 \quad (1)$$

where the sum is conducted over the three interfaces intersecting at the triple junction,  $\sigma_j$  is the excess free energy of the  $j^{\text{th}}$  boundary,  $\hat{n}^{(j)}$  is the unit boundary normal of the  $j^{\text{th}}$  boundary,  $\hat{b}^{(j)}$  is a unit vector lying in the  $j^{\text{th}}$  boundary and perpendicular to the triple line,  $\hat{l} = \hat{n}^{(j)} \wedge \hat{b}^{(j)}$  which is common to all three adjacent boundaries and  $\phi_i$  is defined to be the right handed angle of rotation about triple line of the  $j^{\text{th}}$  boundary from a reference direction. The derivative terms are referred to as torque terms and reflect the dependence of interface energy on orientation about the triple junction.

If the interface energy is independent of interface orientation, Herring's equations reduce to the Young equations:

$$\sigma_1 / \sin(\chi_1) = \sigma_2 / \sin(\chi_2) = \sigma_3 / \sin(\chi_3) \quad (2)$$

Further, a geometrical relationship between boundary migration rates has been described by Adams *et al.* [2] based on the assumption that boundaries migrate only due to their capillarity and that other driving forces are negligible. Then the relation

$$\sum_{i=1,3} M_i [\sin(\chi_i) \sigma_i \kappa_i] = 0 \quad (3)$$

holds, where  $\kappa_i$  is the sum of the two principal curvatures at a triple junction associated with the  $i^{\text{th}}$  grain boundary. The assumptions underlying equation (3) are that the boundary migration rate is linearly related to the driving force  $f (= \sigma \kappa)$  by a proportionality factor  $M$ , representing mobility, and that  $M$  and the energy are independent of the boundary inclination. Thus each triple junction geometry yields two energy-related equations and one mobility-related equation. After characterizing a sufficient number of triple junction geometries, relative boundary energies and mobilities as a function of grain boundary misorientation can be extracted through a statistical/multiscale analysis [4] of equations (2) and (3).

The current size of the data sets is only large enough, however, to allow for the analysis to be executed on the basis of a three-parameter description of grain boundary character. A data set for predominantly low angle boundaries in an aluminum of moderate purity (99.98%) has been analyzed based on misorientation angle and misorientation axis type for both energy and mobility. The results of the one-parameter analysis (angle) are in good agreement with the literature. The

Int. Conf. on Grain Growth and Recrystallization, Aachen, Germany, p165 (2001).

results of the two-parameter analysis (axis) show mild variations in energy with type but strong variations in mobility. The results for energy measurements in magnesia indicate that the conventional view of uniform boundary energy except for low angle boundaries and for well matched lattices, as indicated by a high fraction of coincident lattice sites (low sigma values) is not likely to be true [5]. For a special case of grain boundaries in equilibrium with solid-vapor surfaces in MgO for which one of the torque terms could be neglected, a reconstruction of the *surface energy* has been performed that includes torque terms for the solid-vapor surfaces [6]. The results from this analysis indicate that the torque terms are very important for determination of the map of surface energy. Torque terms arising from the inclination dependence of the boundary energy for internal triple junctions (i.e. between three grain boundaries) will be included in the analysis of (five parameter) grain boundary energy once larger data sets are available.

### **1.b Current Knowledge of Grain Boundary Properties**

Current knowledge of the properties of grain boundaries is limited to special boundary types. Furthermore much of the available literature concerns computer simulation. Thorough reviews by Wolf and Yip and, more recently by Sutton and Baluffi [7] provide excellent overviews of boundary structure and properties. Most experimental determinations of grain boundary energy have relied on a force balance between surface energy and grain boundary energy, e.g. [8]. In contrast to the literature on metals, one of the few contributions on oxides is that of Dhalenne et al. who measured thermal grooves on NiO for boundaries in  $\langle 110 \rangle$  tilt boundaries [9]. Their results indicated little variation in energy for  $\langle 100 \rangle$  high angle tilt boundaries.  $\langle 110 \rangle$  tilt boundaries, however, showed cusps at the  $\Sigma 9$  (221 plane),  $\Sigma 11$  (311 plane) and the (expected)  $\Sigma 3$  positions. The grain boundary energies were higher for  $\langle 110 \rangle$  misorientations than for  $\langle 100 \rangle$  boundaries, although this result assumed constant surface energy. The methods outlined above have been applied by Saylor and Rohrer to measurement of (relative) grain boundary energy in MgO [5], also using thermal grooves. As discussed elsewhere, they also found surface energy to be orientation (inclination) dependent in MgO [6]. More recently Otsuki [10, 11] has conducted a series of experiments on aluminum in which intersections of grain boundaries with a solid-liquid surface were characterized. By assuming a constant solid-liquid interfacial energy and examining a variety of interfaces based on  $\langle 100 \rangle$  and  $\langle 110 \rangle$  rotation axes, information has been obtained on symmetric tilt, asymmetric tilt, twist and mixed character boundaries. The results also showed cusps at the  $\Sigma 11$  (311 plane) and the (expected)  $\Sigma 3$  positions, though not at the  $\Sigma 9$  (221 plane) position. Their results also confirmed previous results for metals, i.e. that twist boundaries tend to have lower energies than the corresponding tilt boundaries. A concern with this approach is that a concentrated alloy is used as the liquid in order to avoid melting the (unalloyed) solid aluminum: solute will diffuse into the solid, especially along boundaries and the presence of the solute may perturb the boundary energy.

The mobility of grain boundaries has been extensively studied since the late 1950s [12, 13, 14, 15, 16] and an excellent review is available in the book by Gottstein and Shvindlerman [17]. Although this introduction cannot do justice to the topic, there is general agreement that low angle boundaries have much lower mobilities than high angle boundaries as a consequence of their discrete dislocation structure. This difference in behavior is also apparent in the generally higher activation energies for low angle boundary mobilities, corresponding to bulk diffusion mechanisms, than for high boundary mobilities. There is also considerable variation in mobility with boundary type for high angle boundaries. As with the case of energy, mobility has been mostly studied for bicrystal specimens containing a single boundary whose type generally close to a low index misorientation axis such as  $\langle 100 \rangle$  or  $\langle 111 \rangle$ . For the series of boundaries based on rotations about a  $\langle 111 \rangle$  axis, simulation using molecular dynamics suggests that the CSL-related boundaries have low energy and high mobility relative to general boundaries. These simulations have been carried out with potentials for aluminum [18, 19]. This limited range of boundary type for which information is available has motivated the present study of grain boundary properties over the whole fundamental zone.

## 2 Experimental Procedure: Al foil

An Al foil sample of purity 99.98% was annealed at 550°C for 9 hours in a N<sub>2</sub> environment. This resulted in a columnar grain structure as observed by optical

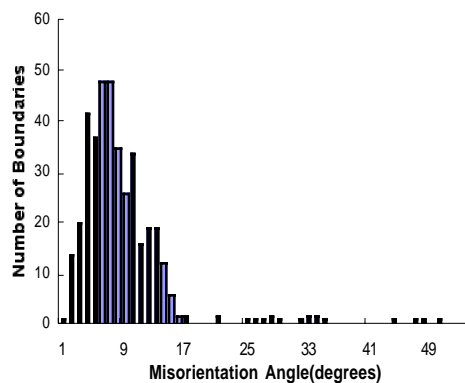


**Fig. 2.** Frequency of boundaries versus misorientation (°)

microscopy. The texture was dominated by a strong cube component,  $\{100\}\langle 001 \rangle$ , with occasional randomly oriented grains. Since the columnar structure results in triple junctions that are nearly straight and perpendicular to the surfaces, the difficulty and error of measuring true dihedral angles and principal curvatures for each grain boundary by the serial sectioning technique is effectively eliminated. Crystallographic information for the grains adjacent to each triple junction was obtained by using orientation imaging microscopy in a scanning electron microscope.

Analysis of the grain boundaries showed a predominance of low angle boundaries, fig. 2. The full five-parameter nature of the boundaries was further analyzed by

locating the boundary plane in a pole figure after determining the disorientation, fig. 3. In this figure, the disorientation is plotted in the small triangular section in Rodrigues space in the lower right corner of each subplot. The first subplot, fig 3a, contains most of the boundaries because of the predominance of low angle boundaries. The boundary planes are plotted in the full circle pole figure (equal area projection), together with the disorientation axis in a unit triangle on the right hand side of the circle. Note that the full range of disorientation vectors is not plotted here because there were so few boundaries with higher values of  $R_3$ . The strong cube texture means that most of the misorientations are close to the origin in Rodrigues space and therefore plot in the first section, 3(a).

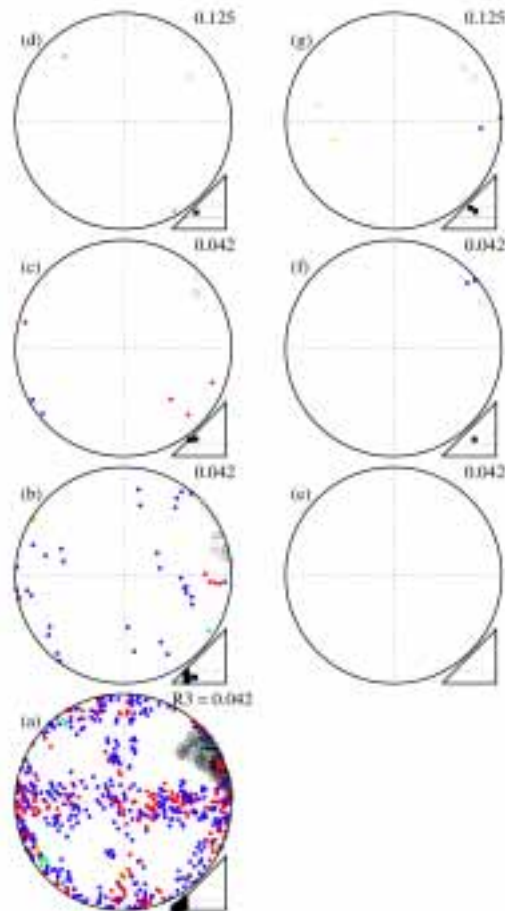


**Fig. 3.** Plot of the grain boundary plane (full circle pole figure in equal area projection) with disorientation (section of Rodrigues space). Most boundaries are low angle boundaries in the first section, 3(a), and the strong  $\{001\}\langle 100\rangle$  texture means that the boundary planes are confined to  $\langle 010\rangle$  zones.

Also the boundary planes are confined to the 001 zone(s) with very few {111} planes present in the sample. In order to extract the dihedral angles and curvatures, each triple junction was recorded on an individual scanning electron micrograph, fig. 4a. Image processing methods [20] were used to skeletonize the grain boundaries, fig. 4b, and curve fitting of a conic section to each boundary [21], fig. 4c, was performed in order to extract the required quantities.

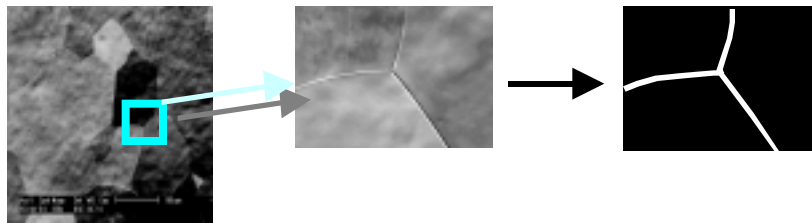


**Fig. 4.** (a) Back scatter contrast scanning electron micrograph of Al foil in plan view. (b) Magnified view of a triple junction. (c) Skeletonized image of boundaries comprising the triple junction in (b).

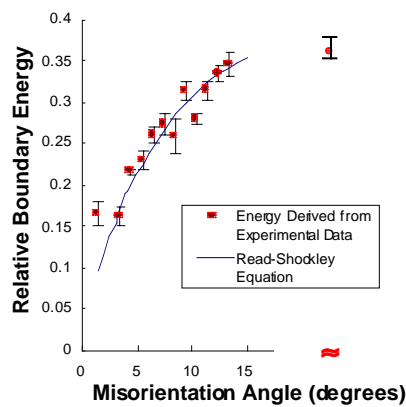


**Fig. 5a.** Plot of grain boundary energy versus misorientation angle (points) with Read-Shockley equation fit (line).

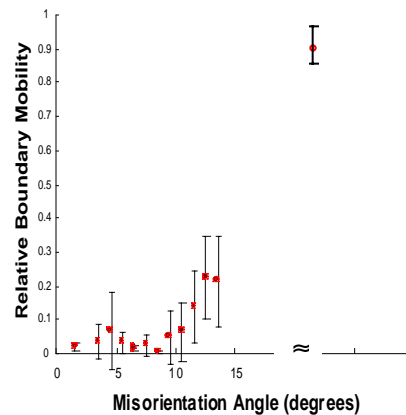


**Fig. 5b.** Plot of grain boundary mobility versus misorientation angle showing sharp transition for angles greater than  $10^\circ$ . The mobilities are scaled by a high angle mobility of one.

### 3. Results

#### 3.1 Measurement of grain boundary energy and mobility in Al: as a function of misorientation angle

402 grain boundaries were characterized at 134 triple junctions in the Al foil. The boundaries were sorted into the 13 different types based on their misorientation angles. The misorientation angle distribution of the boundaries is shown in Fig. 5(a), which shows that most are low angle grain boundaries, *i.e.* misorientation angle  $\theta < 15^\circ$ . The dihedral angles were used as input to the statistical/multiscale analysis [4] to first calculate the grain boundary energy. Error analysis was performed by subdividing the experimental data, *i.e.* sets of triple junctions, into two batches randomly, and comparing the calculation results. Four calculations are performed for both energy and mobility, and we use the interval  $M \pm S$  to represent the experimental result, where  $M$  and  $S$  are the mean and the standard deviation, respectively, of the four associated data sets. Fig. 5(b) shows the variation of relative boundary energy with misorientation angle. For low angle grain boundary energies, the experimental data is fit well with the Read-Shockley equation; the average relative energy for high angle grain boundaries is 0.37. A similar statistical calculation was performed based on equation (3) to obtain grain boundary mobility as a function of misorientation angle as shown in Fig. 5(c). The results show that high angle grain boundaries are much more mobile than low angle boundaries and that there is a sharp transition in mobility in the range 10-15°.

#### 3.2 Measurement of grain boundary energy and mobility in Al: as a function of misorientation axis

In a second analysis, only low angle grain boundaries, *i.e.* boundaries with

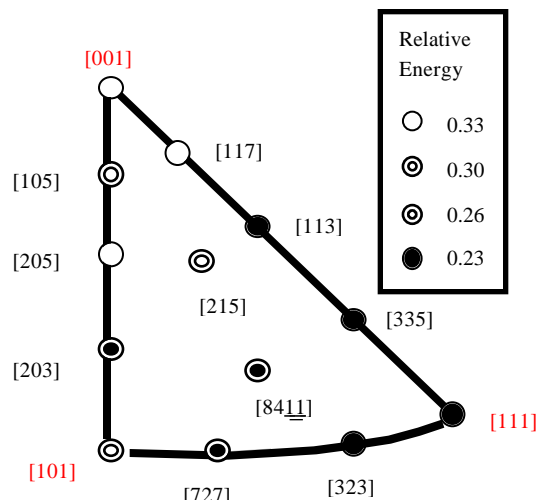


**Fig. 6a.** Variation in grain boundary energy for low angle boundaries as a function of misorientation axis

misorientation angles less than  $15^\circ$ , were included, and the boundaries were relocated to their physically equivalent positions within the fundamental zone, *i.e.* the standard stereographic triangle, 001-101-111. All sorted into 13 different types, chosen to give uniform coverage of the standard stereographic triangle. Each boundary was

assigned to a particular type by finding the nearest axis from the list of 13 types. As for the previous analysis, the resolution was limited by the size of the experimental data set. The same statistical analysis for the calculation of boundary energies and mobilities was performed as used in the previous section

Fig. 6a shows the misorientation axis dependence of the boundary energy. Comparing the three low Miller index axes in the corners of the triangle,  $\langle 001 \rangle$ ,  $\langle 101 \rangle$ , and  $\langle 111 \rangle$ , it was found that  $\sigma_{[001]} \approx \sigma_{[101]} > \sigma_{[111]}$ . Fig.6b shows the variation of low angle boundary mobility with the boundary misorientation axis.  $\langle 111 \rangle$  type boundaries are much more mobile than  $\langle 101 \rangle$  and  $\langle 001 \rangle$  type boundaries, *i.e.*  $M_{[111]} > M_{[101]} \gg M_{[001]}$ . Bauer and Lanxner also theoretically predicted and experimentally demonstrated [22] that boundaries with  $\langle 111 \rangle$  and  $\langle 101 \rangle$  much more mobile than  $\langle 001 \rangle$  type boundaries by a factor of approximately 150, which is consistent with the results of the current work. If

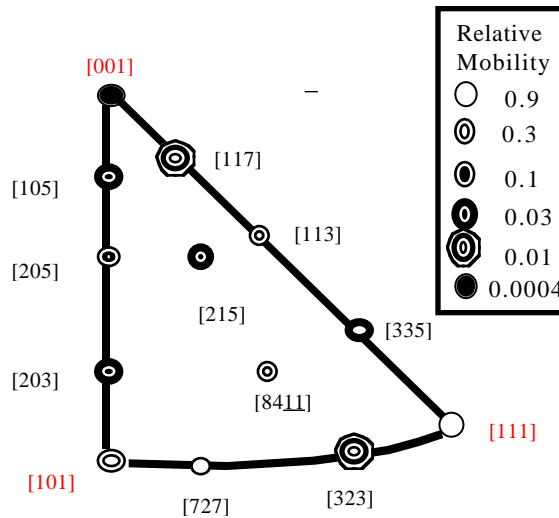


**Fig. 6b.** Variation in grain boundary mobility for low angle boundaries as a function of misorientation axis

diffusion is required in order to advance the boundary and maintain the equilibrium dislocation spacing.

#### 4. Summary

The method of extracting grain boundary energy and mobility from triple junction geometry and crystallography has been demonstrated for a sample of aluminum foil. The foil was annealed in order to produce a columnar grain structure which allowed all the required information to be obtained from a single section. The

symmetric tilt boundaries are considered whose mobility is limited by diffusion between adjacent (parallel) dislocations comprising the boundary, then  $\langle 001 \rangle$  tilt boundaries are seen to be less mobile than either  $\langle 110 \rangle$  or  $\langle 111 \rangle$  tilt boundaries because the Burgers vectors are inclined at approximately  $45^\circ$  to the plane in the former case. In the latter types ( $\langle 110 \rangle$  and  $\langle 111 \rangle$  tilts) the Burgers vectors are nearly normal to the boundary plane which means that much less

Int. Conf. on Grain Growth and Recrystallization, Aachen, Germany, p165 (2001).

strongly (cube) textured material contained a large fraction of low angle boundaries. The variation in energy of these boundaries was found to follow the Read-Shockley equation, with a mild dependence on the misorientation axis. The mobility of the boundaries was found to depend strongly on both misorientation angle and on misorientation axis.

### Acknowledgement

This work was supported primarily by the MRSEC program of the National Science Foundation under Award Number DMR-0079996.

### References

1. B. L. Adams, D. Kinderlehrer, W. W. Mullins, A. D. Rollett and S. Ta'asan, *Scripta mat.*, **38** (1997), pp. 531.
2. C. Herring, *Phys. Rev.*, **82** (1951), pp. 87.
3. C. Herring, in *The Physics of Powder Metallurgy*, W. E. Kingston, Eds. McGraw-Hill Book Co., New York, 1951, pp. 143.
4. D. Kinderlehrer, I. Livshits, S. Ta'asan and D. E. Mason, in *Proc. ICOTOM-12*, Montréal, Canada, J. A. Szpunar, Eds., NRC Research Press, vol. 2, (1999) pp. 1643.
5. D. M. Saylor and G. S. Rohrer, in *Proc. ICOTOM-12*, Montréal, Canada, J. A. Szpunar, Eds., NRC Research Press, vol. 2, (1999) pp. 1690.
6. D. M. Saylor, D. E. Mason and G. S. Rohrer, *J. Am. Ceram. Soc.*, **83** (2000), pp. 1226.
7. A. P. Sutton and R. W. Balluffi, *Interfaces in Crystalline Materials.*, R. J. Brook, et al., Eds., Clarendon Press, Oxford, UK, (1995).
8. N. A. Gjostein and F. N. Rhines, *Acta metall.*, **7** (1959), pp. 319.
9. G. Dhalenne, M. Dechamps and A. Revcolevschi, in *Proc. Advances in Ceramics*, M. F. Yan, A. H. Heuer, Eds., American Ceramic Society, Columbus, OH, vol. 6, (1983) pp. 138.
10. A. Otsuki, *Mater. Sci. Forum*, **207-209** (1996), pp. 413.
11. A. Otsuki, H. Yato and I. Kinjyo, *Mater. Sci. Forum*, **126-128** (1993), pp. 285.
12. J. W. Rutter and K. T. Aust, *Trans. Met. Soc. AIME*, **218** (1960), pp. 682.
13. J. W. Rutter and K. T. Aust, *Acta metall.*, **13** (1960), pp. 181.
14. B. B. Rath and H. Hu, *Trans. Met. Soc. AIME*, **236** (1966), pp. 1193.
15. R. Viswanathan and C. L. Bauer, *Acta metall.*, **21** (1973), pp. 1099.
16. R. C. Sun and C. L. Bauer, *Acta metall.*, **18** (1970), pp. 639.

17. G. Gottstein and L. S. Shvindlerman, Grain Boundary Migration in Metals., CRC Series in Materials Science & Technology CRC Press, Boca Raton, FL, (1999).
18. D. Srolovitz, M. Upmanyu, L. Shvindlerman and G. Gottstein, *Acta mater.*, **47** (1999), pp. 3901.
19. M. Upmanyu, D. Srolovitz and R. Smith, *Int. Sci.*, **6** (1998), pp. 41.
20. A. Talukder, D. Casasent and S. Ozdemir, in Proc. ICOTOM-12, Montréal, Canada, J. A. Szpunar, Eds., NRC Research Press, vol. 1, (1999) pp. 243.
21. C. C. Yang, Extraction of Grain Boundary Energies and Mobilities from Triple Junction Geometry, Ph.D., Carnegie Mellon (2000).
22. C. L. Bauer and M. Lanxner, in Proc. JIMIS-4, Minakami, Japan, Y. Ishida, Eds., Trans. Japan Inst. Metals, vol. 27, (1986) pp. 411.